

Thin Film Maxwell-Power Law Fluid Flow on an Extending Surface

Taza Gul^{1,*}, Zatoon Khan²

¹Government Superior Science College Peshawar, Peshawar, Pakistan

²Oil & Gas Development Company, Peshawar, Pakistan

ARTICLE INFO

Article history:

Received: August 26, 2023

Revised: December 05, 2023

Accepted: December 05, 2023

Published: December 30, 2023

Keywords:

Maxwell-Power-law fluid

Magnetohydrodynamics (MHD)

Nanofluid thin film

Darcy-Forchheimer flow

Homotopy Analysis Method (HAM)

ABSTRACT

In this research article, the examination is done on two-dimensional fluid film flow and heat transfer with a magnetic field on an unsteady extending sheet. To gain the appropriate outputs for the flow efficiency and heat transfer rate the Power law fluids are mixed with the viscoelastic fluids which reduces the viscosity of the fluids. The heat transfer rate is further improved with the inclusion of nanoparticles. The flow and heat transmission characteristics of a Maxwell/Power-law model fluid with Joule absorption and changeable liquid sheet thickness are examined. The combined model of the two non-Newtonian fluids also incorporated the nanofluid's influence. To create the coupled comparable ordinary differential equations (ODEs) that the homotopy analytical method (HAM) along with appropriate similarity transformations are used. Impacts of variations of different significant factors like Cf_x and Nu number for fluid flow of liquid film with transfer of heat are perceived. The influence of unsteadiness factor S over thin film is discovered analytically for various estimations. Moreover, the implanted factors utilized for understanding of the physical demonstration, like magnetic factor M , inertial parameter F_1 , Eckert number Ec , penetrability factor K_1 , Prandtl number Pr and Deborah number De have been offered by graphs and deliberated in detail.

1 Introduction

Because of "Nanofluid's" excellent thermal conductivity and innovative uses in numerous fields of science, engineering, and technology, researchers have been paying a lot of attention to it during the past 20 years. The limited thermal conductivity of common liquids makes them unsuitable for a number of heat transfer problems. However, the metal has a well-known high heat conductivity. Consequently, the mixing of metal and a regular fluid appears to increase the resultant thermal conductivity, and Masuda et al. [1] were the first to identify this peculiar phenomenon. Choi [2] subsequently referred to the unique structure as a nanofluid. The term "nanofluid" describes a uniform solution of base fluids such as ethylene glycol, kerosene, water, etc. with minute metallic particles (5-100nm in size). Nanofluids' noble properties, such as their exceptional thermal conductivity, minimal congesting, robust stability, and homogeneity, appreciated them as a commonly accepted form of media in a variety of industries, such as chemical production, electronics, production, automotive, medical therapy, solar collectors, and nuclear systems [3-5].

Many scholars have documented using a wide range of numerical and theoretical models to depict the unusual increase in thermal conductivity. Convective nanofluidic transmission was discussed by Buongiorno [6] while taking Brownian motion and thermophoresis into account. He discovered throughout

*Corresponding author: Taza Gul
email address: tazagulaworkum@gmail.com



his research that thermophoretic and Brownian diffusions are the main causes of the remarkable increase in heat transport of nanofluid. Tiwari and Das [7] modeled the heat transport process of nanofluid by adding the size distribution, thermal conductivity, viscosity, and volume fraction. The natural convective nanofluid flow within a porous layer was studied by Nield and Kuznetsov [8]. The mass and heat transport characteristics of radiative flow of nanofluid within a rotating annulus were shown by Peng et al. [9]. They noticed that radiation causes the rate of heat transmission to increase. The ethylene glycol-based flow of Ferrofluid on a stretched surface was examined by Khan et al. [10]. They discovered that ethylene glycol performs far stronger as a host fluid than water. The unstable compressing nanofluid flow between parallel surfaces was studied by Sheikholeslami et al. [11]. According to their findings, heat transfer increases with nanoparticle concentration.

Nomenclature

Description	Symbols	Description	Symbols
Fluid Temperature	T	Fluid Velocity	$V = (u, v)$
Slit Temperature	T_0	Cartesian coordinates	(x, y)
Extra tensor	S	RivlinEriksen tensor	A
Positive reverence temperature	T_{ref}	Initial stretching sheet	b
Prandle number	Pr	Eckert number	Ec
Thermal conductivity of nanofluid	k_{nf}	Deborah number	De
Unsteady parameter	S	Maragoni number	M_1
Positive constant	α	Magnetic field parameter	M
Consistency thermal coefficient	k_0	Surface tension of the slit	σ_0
Dimensionless film thickness	β	Dimensionless temperature	θ
Uniform thin film thickness	$h(x, t)$	Surface tension	σ_1
Dimensionless velocity	f'	Nanofluid Density	ρ_{nf}
Applied magnetic field	β_0	Temperature coefficient	$\dot{\gamma}$
Nanofluid Thermal diffusivity	α_{nf}	Nanofluid Dynamic viscosity	μ_{nf}
Similarity variable	η	Relaxation time	λ
Power law index	n	Nanofluid Kinematic viscosity	ν_{nf}
Nanofluid Electrical conductivity	σ_{nf}	Differentiate with respect to η	'

MHD nanofluidic movement over a porous extendable surface was demonstrated by Alam et al. [12]. They noticed a drop in temperature due to instability. The Hall and slip effects on the erratic rotating flow of nanofluid were demonstrated by Krishna and Chamkha [13]. Findings showed that the concentration of nanoparticles increases skin friction. Ramzan et al. [14] examined the flow of a radiative ethylene glycol-based carbon nanotube between two rotating discs. They noted that the concentration of nanoparticles increases temperature and radial velocity.

By using a stretching sheet, Hassaniien et al. [15] looked into the fluid flow across a plate while applying a power law model. For the fluid across a stretching sheet, Rao et al. [16] have also employed the power law model. Abel et al. [17] examined the power law model liquid with changing thermal conductivity improving the thermal efficiency. Chen [18], studied the power law liquid along with the impact of magnetic field. The related results can be seen in [19, 20]. The thin film flow was examined by Zhang et al. [21] while using the Power law model. Bai et al. [22] have studied the nanofluid's flow across the stretched surface at its stagnation point when there is a thermophoresis action. The thin film flow was examined by Zhang et al. [21] while using the Power law model. Bai et al. [22] have studied the nano fluid's flow across the stretched surface at its stagnation point when there is a thermophoresis action.

The provision of everyday life employing fluid components, such as food processing, biological fluid motion, electronic chips, extruded processes, and so on, depends heavily on non-Newtonian fluids [25–27]. For viscoelastic fluids like Maxwell fluid, the shear thinning effect is particularly crucial to achieving the desired results for a variety of engineering phenomena, such as hydraulic estimates and a reduction in pumping rates. Additionally, the flow performance of the viscoelastic fluids is enhanced by highly shear thinning fluids (fluids with a power law model). As a result, we chose the existing system employing the Power law and Maxwell fluid combinations [28]. The boundary-layer theory has been put forth by Schowalter [29] in the context of the non-Newtonian power-law liquids hypothesis. The constant laminar motion of non-Newtonian liquids over a plate has been studied by Acrovos et al. The momentum and heat transmission on a continuously moving surface in a power-law liquid have been taken into consideration by Howell et al. [31] and Rao et al. [32].

We examine the thin film Maxwell-Power-law fluid flow across an extended unstable sheet as inspired by the aforesaid literature. According to the innovative studies of Ionesco et al. [33], the inclusion of Power law model fluid and Maxwell fluids is utilized to decline the viscosity of the resulting fluid. They made use of the formal testing of viscoelastic fluid properties (Power law model fluids). Nguyen et al. [34], investigation of viscoelastic fluid flow in a confined circular space added to the field's knowledge. The magnetic field, joule heating, the permeable medium (Darcy Forchheimer) has been included to model the flow. Moreover, a thin coating of nanoliquid has been added to exhibit improved flow thermal behavior. The small nanomaterial's have notable uses in medical applications, medication delivery, solar cells, bio sensing, tissue engineering, cancer treatment, etc. The fundamental equations are transformed into dimensionless form and analytically resolved. To enhance the evaluation, many graphs and tables are displayed. Such unexpected results, in our opinion, will improve nano science.

2 Problem Formulation

The Maxwell-power-law model's thin film flow across an extended, unstable surface with changing thickness has been taken into consideration.

The Darcy-Forchheimer flow is subjected to a vertical application of the magnetic field and $B(t) = B_0(1 - \alpha t)^{-\frac{1}{2}}$. $\vec{U}_w(x, t) = \frac{bx^{\frac{2n}{n+1}}}{(1 - \alpha t)}$, is the prolonging surface's time-varying stretching velocity, while b is the stretching restriction. The basic flow is presented as:

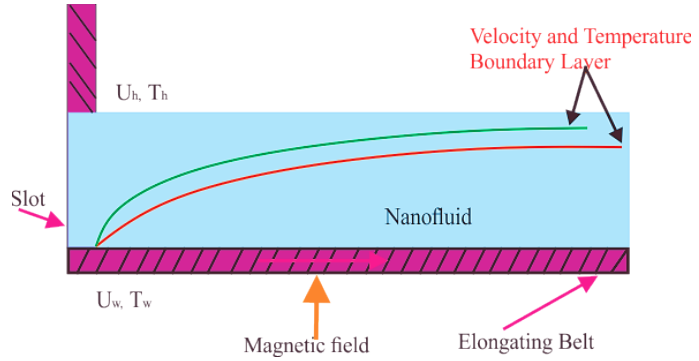


Figure 1: Geometry of the problem

$$\frac{\partial u}{\partial x} + \frac{\partial v}{\partial y} = 0, \quad (1)$$

$$\begin{aligned} \frac{\partial u}{\partial t} + u \frac{\partial u}{\partial x} + v \frac{\partial u}{\partial y} + \lambda_1 \left(u^2 \frac{\partial^2 u}{\partial x^2} + v^2 \frac{\partial^2 u}{\partial y^2} + 2uv \frac{\partial^2 u}{\partial x \partial y} \right) \\ + \frac{\sigma B^2(t)}{\rho_{nf}} u - v_{nf} \frac{u}{k^*} - \frac{C_p}{\rho_{nf} x \sqrt{k^*}} u^2 = v_{nf} \frac{\partial^2 u}{\partial y^2} \frac{\partial}{\partial y} \left(\frac{\partial u}{\partial y} \left| \frac{\partial u}{\partial y} \right|^{n-1} \right), \end{aligned} \quad (2)$$

$$(\rho C_p)_{nf} \left(\frac{\partial T}{\partial t} + u \frac{\partial T}{\partial x} + v \frac{\partial T}{\partial y} \right) + \sigma B^2(t) u^2 = k_{nf} \frac{\partial}{\partial y} \left(|u_y|^{n-1} \frac{\partial T}{\partial y} \right). \quad (3)$$

These are the thermo - physical requirements:

$$\begin{aligned} (\rho C_p)_{nf} &= (1 - \phi) (\rho C_p)_f + \phi (\rho C_p)_s, \quad \rho_{nf} = (1 - \phi) \rho_f + \phi \rho_s, \\ \frac{k_{nf}}{k_f} &= \frac{k_s + 2k_f - 2\phi(k_f - k_s)}{k_s + 2k_f + 2\phi(k_f - k_s)}, \quad \mu_{nf} = \frac{\mu_f}{(1 - \phi)^{2.5}}. \end{aligned} \quad (4)$$

The ratio of the surface area to the volume is very large for thin film with free surface.

The boundary conditions:

$$\begin{aligned} u = U_w, v = 0, T = T_w, \quad \text{at } y = 0; \\ v = u \frac{\partial h}{\partial x} + \frac{\partial h}{\partial t}, \frac{\partial u}{\partial y} = \frac{\partial T}{\partial y} = 0, \quad \text{at } y = h(x, t). \end{aligned} \quad (5)$$

In the reference [15], the stream function and matching transformations are addressed:

$$\begin{aligned} \eta = b^{\frac{2-n}{n+1}} v_f^{-\frac{1}{n+1}} (1 - \alpha t)^{\frac{n-2}{n+1}} y, \quad \psi = b^{\frac{2n-1}{n+1}} v_f^{\frac{1}{n+1}} x^{\frac{2n}{n+1}} (1 - \alpha t)^{\frac{1-2n}{n+1}} f(\eta), \quad u = \psi_y, v = -\psi_x \\ T = T_0 + T_{ref} b x^{\frac{3n+1}{n+1}} (1 - \alpha t)^{-\frac{3n}{n+1}} \Theta(\eta), \quad \beta = h(x, t) b^{\frac{2-n}{n+1}} v_f^{-\frac{1}{n+1}} x^{\frac{1-n}{n+1}} (1 - \alpha t)^{\frac{n-2}{n+1}}. \end{aligned} \quad (6)$$

The ordinary differential equations can be created using Eqs. (5, 6) and Eq. (1):

$$S \left(f' - \eta \frac{n-2}{n+1} f'' \right) + \left(\frac{2n}{n+1} \right) (f'^2 - f f'') + De \left[\frac{4n^2}{(n+1)^2} f^2 f''' - \frac{8n}{(n+1)^2} f f' f'' \right] + \frac{\sigma_f}{\rho_f} M f' + \frac{\nu_{nf}}{\rho_f} k_1 f' + \frac{F_1}{\rho_f} f'^2 = \varepsilon_1 \left(|f''|^{n-1} f'' \right)', \quad (7)$$

$$S \left(\frac{3n}{n+1} \Theta - \eta \left(\frac{n-2}{n+1} \right) \Theta' \right) + \left[\left(\frac{3n+1}{n+1} \right) f' \Theta + \frac{1-n}{1+n} f \Theta' \right] + MEc \Theta f'^2 = \frac{1}{Pr} \varepsilon_2 \left[|f''|^{n-1} \Theta' \right]', \quad (8)$$

when similarity transformations are used:

$$f'(0) = 1, f(0) = 0, \Theta(0) = 1, f(\beta) = \frac{2-n}{2n} S\beta, f''(\beta) = 0, \Theta'(\beta) = 0, \quad (9)$$

The value of ε_1 and ε_2 are given below from reference [10]:

$$\varepsilon_1 = \frac{1}{(1-\phi)^{2.5} [(1-\phi) + \phi \rho_s / \rho_f]}, \varepsilon_2 = \frac{k_{nf} / k_f}{[(1-\phi) + \phi (\rho C_p)_s / (\rho C_p)_f]}. \quad (10)$$

The equations of C_f , and Nu_x , are given as:

$$C_f = - \left(\frac{\tau_w}{\rho_f \frac{U_w^2}{2}} \right)_{y=0}, Nu_x = - \left(\frac{q_w x}{k_f (T_w - T_0)} \right)_{y=0}. \quad (11)$$

2.1 Solution by HAM

The HAM approach is used to resolve the issue [35–40]. The equations that make up the flow must be solved using the HAM method in the mathematica software. The following are the initial presumptions.

$$\hat{f}_0(\eta) = \frac{3}{2n\beta^2} [2n - S(2-n)] \left[\frac{\eta^3}{6} - \frac{\eta^2\beta}{2} \right] + \eta, \Theta_0(\eta) = 1, \quad (12)$$

$L_{\hat{f}}, L_{\hat{\theta}}$ denoted the linear operators

$$L_{\hat{f}}(\hat{f}) = \hat{f}''', L_{\hat{\theta}}(\hat{\theta}) = \hat{\theta}''', \quad (13)$$

which have

$$L_{\hat{f}}(e_1 + e_2\eta + e_3\eta^2) = 0, L_{\hat{\theta}}(e_4 + e_5\eta) = 0, \quad (14)$$

here e_1, e_2 and e_3 are constants.

The equivalent non-linear operators $N_{\hat{f}}, N_{\hat{\theta}}$ are nominated in the form:

$$N_{\hat{f}} \left[\hat{f}(\eta; \zeta) \right] = S \left(\hat{f}' - \eta \frac{n-2}{n+1} \hat{f}'' \right) + \left(\frac{2n}{n+1} \right) \left(\hat{f}'^2 - \hat{f} \hat{f}'' \right) + De \left[-\frac{8n}{(n+1)^2} \hat{f} \hat{f}' \hat{f}'' + \frac{4n^2}{(n+1)^2} \hat{f}^2 \hat{f}''' \right] + \frac{\sigma_f}{\rho_f} M \hat{f}' + \frac{\nu_{nf}}{\rho_f} k_1 \hat{f}' + \frac{F_1}{\rho_f} \hat{f}'^2 = \left(|\hat{f}''|^{n-1} \hat{f}'' \right)', \quad (15)$$

$$N_{\hat{\theta}} \left[\hat{f}(\eta; \zeta), \hat{\theta}(\eta; \zeta) \right] = S \left(\frac{3n}{n+1} \hat{\theta} - \eta \left(\frac{n-2}{n+1} \right) \hat{\theta}' \right) + \left[\left(\frac{3n+1}{n+1} \right) \hat{f}' \hat{\theta} + \frac{1-n}{1+n} \hat{f} \hat{\theta}' \right] + MEc \hat{\theta} \hat{f}'^2 = \frac{1}{Pr} \varepsilon_2 \left[|\hat{f}''|^{n-1} \hat{\theta}' \right]'. \quad (16)$$

3 Results and Discussion

The results of the extensive calculations to look at the effects of the physical parameters $n, S, M, De, F_1, k_1, Ec, n$, and Pr are shown in figures 2 to 10 for the dimensionless temperature and velocity profile. According to figures 2 and 3, an increase in the parameter M gives a decrease in the velocity for both fluids, Newtonian and non-Newtonian, and an inverse relationship for the temperature profile. This is brought on by the Lorentz force, which opposes forces that act in the same direction as

the flow. This force that opposes causes the fluid's velocity to slow down and its temperature to rise. The profiles of temperature, and velocity in dimensionless form as a function of changing n , the index of power-law, are shown in Figs. 4 and 5. An increment in n causes the thin film thickness to grow. Besides that, as n rises, the dispersion of temperature and velocity decrease. Figs. 6 and 7 show the effects of an unsteady component on the fluid velocity and temperature curves. The results demonstrate that the unsteady components can significantly increase the temperature and fluid velocity. Also, it has been discovered that as S gets stronger, the area between two nearby profiles grows atypically. Physically, the Deborah number represents the ratio of relaxation time with observation time.

A delayed recuperation process forms when De rises along with the relaxation time. As a result, the film's thickness decreases. That is to imply, that elasticity provides flow resistance. The fluid can change into a totally viscous fluid when $De = 0$. The impact of an inertial component on flow velocity is shown in Fig. 9. There are small but noticeable variations in the values of F_1 degradation velocity profile readings. Apparently, there is a rise in porous openings in the porous medium with a growth in the inertial factor. This physical process makes the viscous involvement more intense and finally results in stream channel restriction. Also, as seen in the picture, F_1 has very little of an effect on the dispersion of the velocity of the free stream. Figure 10 shows how the porosity component k_1 affects the velocity distribution. This is definitely understandable as an increase in the estimation of k_1 increases the permeability voids in the material, which creates an antagonism in the streamlines and ultimately decreases the momentum of the nano-fluid and thickness of the associated boundary layer. The velocity curve as shown in Fig. 11 declines with increasing nanoparticle volume fraction ϕ . In actuality, the declining velocity field and rising value of ϕ are what create the opposing force.

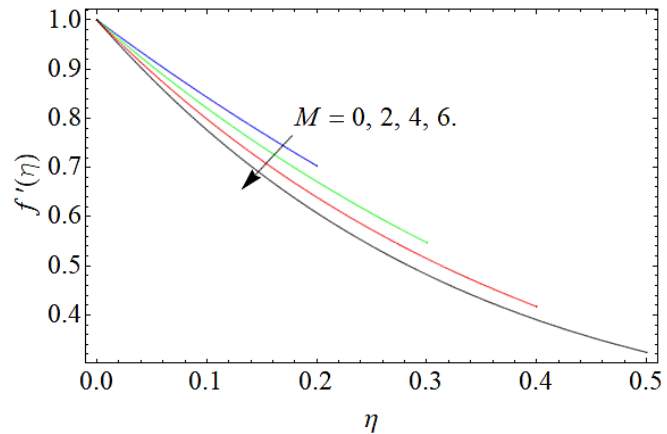


Figure 2: Outcomes of M against $f(\eta)$

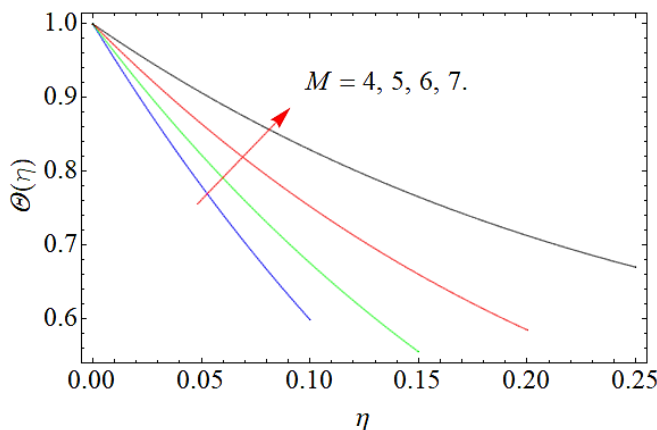


Figure 3: Outcomes of M against $\theta(\eta)$

particle rises in quantity. A bigger number of ϕ physically results in a higher thermal performance, which raises the thermal properties. Different tables are assembled to exhibit the numerical effects of some physical factors. Table. 1 and 2 elucidate the influence of drag force and rate of transfer of heat under the effect of dissimilar factors. The characteristics of S , De , Mon on skin friction for the various estimations have appeared in Table. 1. It is inspected that the expanding rates of M , De and unsteady factor S raise the Skin-friction coefficient. The impacts of S , Pr , Ec on the heat transfer rate for the dissimilar estimations are mentioned in Table 2. It is anticipated that corporate rates of unsteady parameter S and

The effect of Eckert numbers Ec on temperature is shown in Fig. 12. It can be shown that the heated thermal energy of the Maxwell power-law liquid has increased as a result of the improvement in Ec . Ec really stands for the impacts of heat conduction. When heat convection rises and thermal conduction decreases in this physical process of heat transfer, a spike in Ec raises the temperature of the nanofluid. According to Fig. 13, Pr climbs leading to a reduction in heat diffusion, which leads to a drop in temperature. Pr represents the relationship between kinematic viscosity and thermal diffusivity. The temperature distribution shown in Fig. 14 is rising as the volume fraction ϕ of nanoparticle

E increases the heat transfer rate. While the heat transfer rate decreases with the increasing values of Pr .

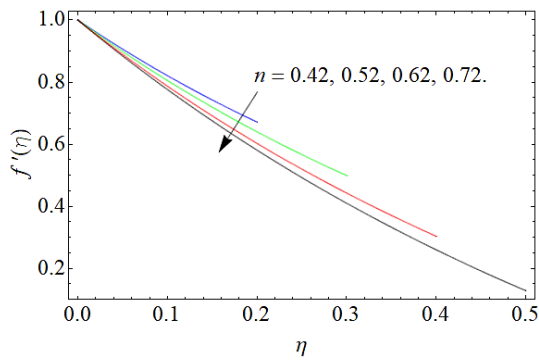


Figure 4: Outcomes of n against $f(\eta)$

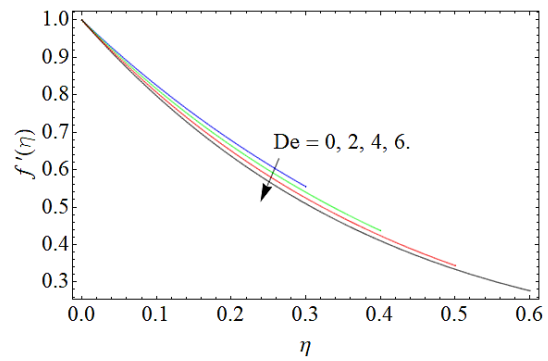


Figure 8: Outcomes of De against $f(\eta)$

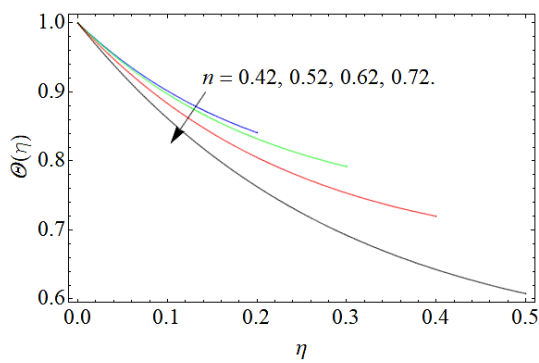


Figure 5: Outcomes of n against $\Theta(\eta)$

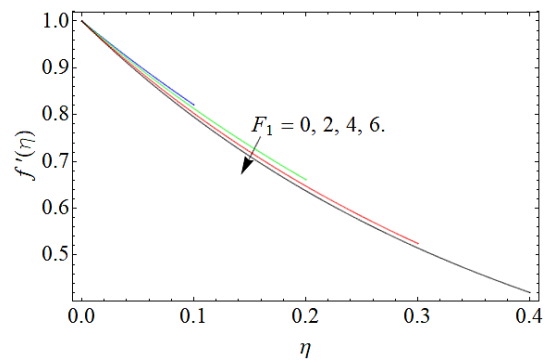


Figure 9: Outcomes of F_1 against $f(\eta)$

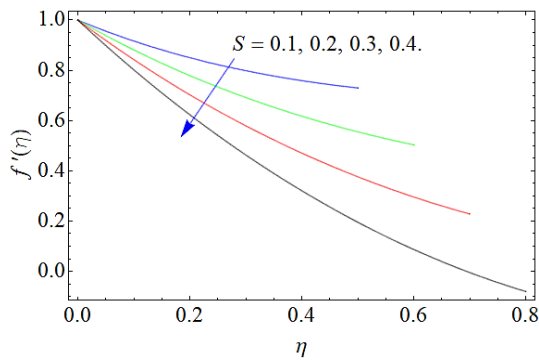


Figure 6: Outcomes of S against $f(\eta)$.

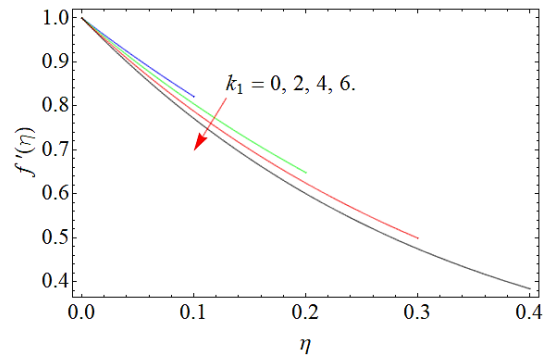


Figure 10: Outcomes of k_1 against $f(\eta)$

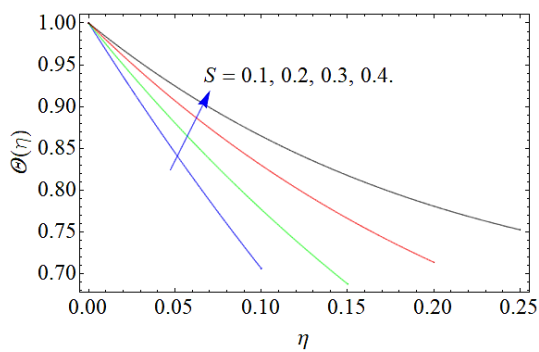


Figure 7: Outcomes of S against $f(\eta)$.

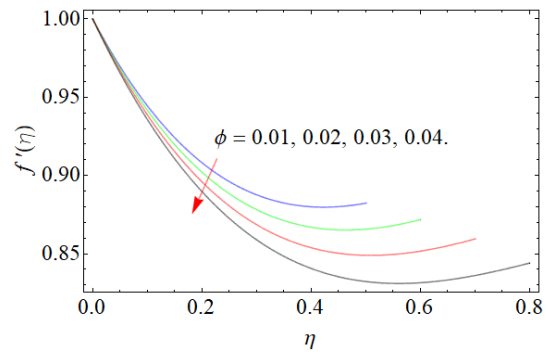


Figure 11: Outcomes of ϕ against $f'(\eta)$

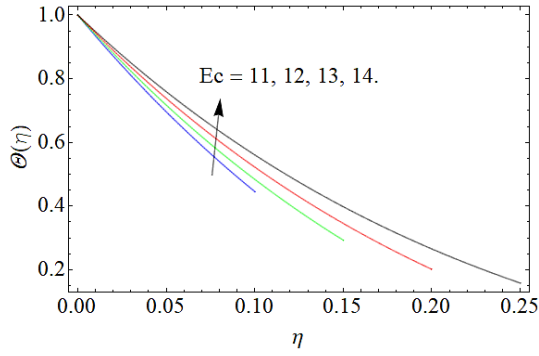


Figure 12: Outcomes of Ec on $\Theta(\eta)$

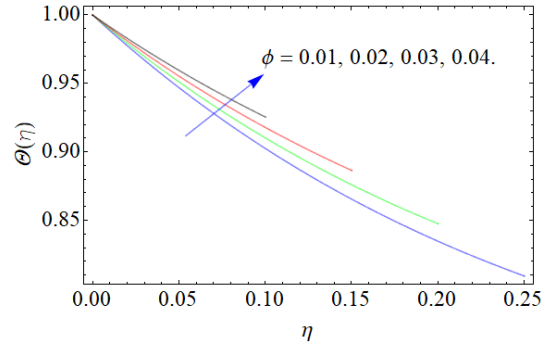


Figure 14: Outcomes of ϕ against $\Theta(\eta)$

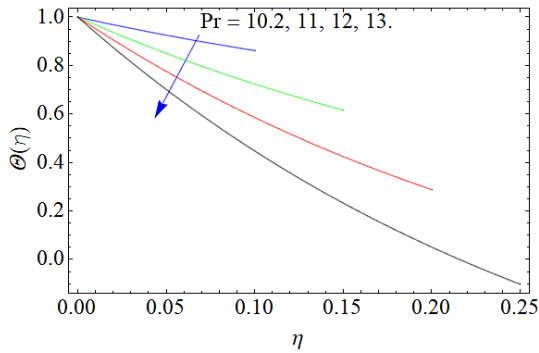


Figure 13: Outcomes of Pr against $\Theta(\eta)$

Table 1: Outcomes of skin friction against different parameters

$f''(0)$	S	De	M
1.57071	0.1	0.3	2
1.58224	0.2		
1.59411	0.3		
1.60632	0.4		
1.59098		0.4	
1.60187		0.5	
1.61326		0.6	
1.595776			3
1.60854			4
1.62168			5

Table 2: Heat transfer rate against different parameters

$\Theta'(0)$	Ec	Pr	S
1.0937	2	10.5	0.1
1.18605			0.2
1.2777			0.3
1.549704			0.4
1.644402	3		
1.73456	4		
1.79879	5		
1.45876		11	
1.34280		11.5	
1.28342		12	

4 Conclusions

Investigations are made into the Maxwell-power-law characteristics of heat transfer and fluid flow with varying layer thickness. The main findings of the investigation presented here can be summed up as follows:

1. The film thickness falls as the unsteadiness parameter increases, which causes the inner velocity of thin films to exceed the surface velocity. This enhances the fluid's stretching velocity, which in turn causes the velocity profile to rise as the unsteadiness parameter's values rise.
2. Increase in the magnetic parameter results in the growth of Lorentz force which offers a resistance to the flow of fluid. Hence growing values of magnetic field declines flow characteristics.
3. Fluid velocity dispersion is reduced when the inertial/Forchheimer parameter is increased. Besides that, because the porosity parameter has a negative impact on the velocity profile, velocity is likewise a lowering function of that quantity.

4. The variations of M_1 show an increment in the temperature of the film.
5. The thickness of the film is definitely altered by the elasticity and viscosity of the nanofluid thin film. That is, the thickness decreases with increasing Deborah number D_e or decreasing power-law index n .
6. For larger estimates of the Eckert number, an increase in the temperature field is shown, and vice versa.

Funding statement The author(s) received no specific funding for this study.

Conflicts of Interest The authors declare no conflict of interest.

References

- [1] H. Masuda, A. Ebata, K. Teramae, and N. Hishinuma, "Alteration of Thermal Conductivity and Viscosity of Liquid by Dispersing Ultra-Fine Particles. Dispersion of Al₂O₃, SiO₂ and TiO₂ Ultra-Fine Particles.," *Netsu Bussei*, vol. 7, no. 4, pp. 227–233, 1993.
- [2] C. Sus, "Enhancing thermal conductivity of fluids with nanoparticles, developments and applications of non-Newtonian flows," *ASME, FED, MD*, 1995, vol. 231, pp. 99-105, 1995.
- [3] M. Hemmat Esfe and M. Afrand, "A review on fuel cell types and the application of nanofluid in their cooling," *J. Therm. Anal. Calorim.*, vol. 140, pp. 1633–1654, 2020.
- [4] O. Z. Sharaf, R. A. Taylor, and E. Abu-Nada, "On the colloidal and chemical stability of solar nanofluids: From nanoscale interactions to recent advances," *Phys. Rep.*, vol. 867, pp. 1–84, 2020.
- [5] O. Z. Sharaf et al., "Ultrastable plasmonic nanofluids in optimized direct absorption solar collectors," *Energy Convers. Manag.*, vol. 199, p. 112010, 2019.
- [6] J. Buongiorno, "Convective transport in nanofluids," 2006.
- [7] R. K. Tiwari and M. K. Das, "Heat transfer augmentation in a two-sided lid-driven differentially heated square cavity utilizing nanofluids," *Int. J. Heat Mass Transf.*, vol. 50, no. 9–10, pp. 2002–2018, 2007.
- [8] D. A. Nield and A. V. Kuznetsov, "The Cheng–Minkowycz problem for natural convective boundary-layer flow in a porous medium saturated by a nanofluid," *Int. J. Heat Mass Transf.*, vol. 52, no. 25–26, pp. 5792–5795, 2009.
- [9] Y. Peng, A. S. Alsagri, M. Afrand, and R. Moradi, "A numerical simulation for magnetohydrodynamic nanofluid flow and heat transfer in rotating horizontal annulus with thermal radiation," *RSC Adv.*, vol. 9, no. 39, pp. 22185–22197, 2019.
- [10] A. Khan, T. Gul, Z. Zaheer, and I. S. Amiri, "The flow of ferromagnetic nanofluid over an extending surface under the effect of operative Prandtl model: a numerical study," *Adv. Mech. Eng.*, vol. 11, no. 12, p. 1687814019896128, 2019.
- [11] M. Sheikholeslami, D. D. Ganji, and H. R. Ashorynejad, "Investigation of squeezing unsteady nanofluid flow using ADM," *Powder Technol.*, vol. 239, pp. 259–265, 2013.
- [12] M. S. Alam, M. Ali, M. A. Alim, and M. J. Munshi, "Unsteady boundary layer nanofluid flow and heat transfer along a porous stretching surface with magnetic field," in *AIP conference proceedings*, 2017, vol. 1851, no. 1.
- [13] M. V. Krishna and A. J. Chamkha, "Hall and ion slip effects on Unsteady MHD Convective Rotating flow of Nanofluids—Application in Biomedical Engineering," *J. Egypt. Math. Soc.*, vol. 28, no. 1, p. 1, 2020.
- [14] M. Ramzan, S. Riasat, Z. Shah, P. Kumam, and P. Thounthong, "Unsteady MHD carbon nanotubes suspended nanofluid flow with thermal stratification and nonlinear thermal radiation," *Alexandria Eng. J.*, vol. 59, no. 3, pp. 1557–1566, 2020.

- [15] I. A. Hassanien, A. A. Abdullah, and R. S. R. Gorla, "Flow and heat transfer in a power-law fluid over a nonisothermal stretching sheet," *Math. Comput. Model.*, vol. 28, no. 9, pp. 105–116, 1998.
- [16] J. H. Rao, D. R. Jeng, and K. J. De Witt, "Momentum and heat transfer in a power-law fluid with arbitrary injection/suction at a moving wall," *Int. J. Heat Mass Transf.*, vol. 42, no. 15, pp. 2837–2847, 1999.
- [17] M. S. Abel, P. S. Datti, and N. Mahesha, "Flow and heat transfer in a power-law fluid over a stretching sheet with variable thermal conductivity and non-uniform heat source," *Int. J. Heat Mass Transf.*, vol. 52, no. 11–12, pp. 2902–2913, 2009.
- [18] C.-H. Chen, "Magneto-hydrodynamic mixed convection of a power-law fluid past a stretching surface in the presence of thermal radiation and internal heat generation/absorption," *Int. J. Non. Linear. Mech.*, vol. 44, no. 6, pp. 596–603, 2009.
- [19] X. Si, X. Zhu, L. Zheng, X. Zhang, and P. Lin, "Laminar film condensation of pseudo-plastic non-Newtonian fluid with variable thermal conductivity on an isothermal vertical plate," *Int. J. Heat Mass Transf.*, vol. 92, pp. 979–986, 2016.
- [20] Y. Zhang, M. Zhang, and Y. Bai, "Unsteady flow and heat transfer of power-law nanofluid thin film over a stretching sheet with variable magnetic field and power-law velocity slip effect," *J. Taiwan Inst. Chem. Eng.*, vol. 70, pp. 104–110, 2017.
- [21] Y. Zhang, M. Zhang, and Y. Bai, "Unsteady flow and heat transfer of power-law nanofluid thin film over a stretching sheet with variable magnetic field and power-law velocity slip effect," *J. Taiwan Inst. Chem. Eng.*, vol. 70, pp. 104–110, 2017.
- [22] Y. Bai, X. Liu, Y. Zhang, and M. Zhang, "Stagnation-point heat and mass transfer of MHD Maxwell nanofluids over a stretching surface in the presence of thermophoresis," *J. Mol. Liq.*, vol. 224, pp. 1172–1180, 2016.
- [23] R. Jusoh, R. Nazar, and I. Pop, "Flow and heat transfer of magnetohydrodynamic three-dimensional Maxwell nanofluid over a permeable stretching/shrinking surface with convective boundary conditions," *Int. J. Mech. Sci.*, vol. 124, pp. 166–173, 2017.
- [24] M. Jawad, Z. Shah, S. Islam, W. Khan, and A. Z. Khan, "Nanofluid thin film flow of Sisko fluid and variable heat transfer over an unsteady stretching surface with external magnetic field," *J. Algorithm. Comput. Technol.*, vol. 13, p. 1748301819832456, 2019.
- [25] K. V. Prasad, S. R. Santhi, and P. S. Datti, "Non-Newtonian power-law fluid flow and heat transfer over a non-linearly stretching surface," 2012.
- [26] J. Wu and M. C. Thompson, "Non-Newtonian shear-thinning flows past a flat plate," *J. Nonnewton. Fluid Mech.*, vol. 66, no. 2–3, pp. 127–144, 1996.
- [27] D. Vieru, C. Fetecau, and C. Fetecau, "Flow of a viscoelastic fluid with the fractional Maxwell model between two side walls perpendicular to a plate," *Appl. Math. Comput.*, vol. 200, no. 1, pp. 459–464, 2008.
- [28] R. Caenn, H. C. H. Darley, and G. R. Gray, *Composition and properties of drilling and completion fluids*. Gulf professional publishing, 2011.
- [29] W. R. Schowalter, "The application of boundary-layer theory to power-law pseudoplastic fluids: Similar solutions," *AIChE J.*, vol. 6, no. 1, pp. 24–28, 1960.
- [30] A. Acrivos, M. J. Shah, and E. E. Petersen, "Momentum and heat transfer in laminar boundary-layer flows of non-Newtonian fluids past external surfaces," *AIChE J.*, vol. 6, no. 2, pp. 312–317, 1960.
- [31] T. G. Howell, D. R. Jeng, and K. J. De Witt, "Momentum and heat transfer on a continuous moving surface in a power law fluid," *Int. J. Heat Mass Transf.*, vol. 40, no. 8, pp. 1853–1861, 1997.
- [32] J. H. Rao, D. R. Jeng, and K. J. De Witt, "Momentum and heat transfer in a power-law fluid with arbitrary injection/suction at a moving wall," *Int. J. Heat Mass Transf.*, vol. 42, no. 15, pp. 2837–2847, 1999.

- [33] C.-M. Ionescu, I. R. Birs, D. Copot, C. I. Muresan, and R. Caponetto, “Mathematical modelling with experimental validation of viscoelastic properties in non-Newtonian fluids,” *Philos. Trans. R. Soc. A*, vol. 378, no. 2172, p. 20190284, 2020.
- [34] T. Nguyen, D. van der Meer, A. van den Berg, and J. C. T. Eijkel, “Investigation of the effects of time periodic pressure and potential gradients on viscoelastic fluid flow in circular narrow confinements,” *Microfluid. Nanofluidics*, vol. 21, pp. 1–12, 2017.
- [35] S.-J. Liao, “The proposed homotopy analysis technique for the solution of nonlinear problems.” PhD thesis, Shanghai Jiao Tong University China, 1992.
- [36] S. Liao, “On the homotopy analysis method for nonlinear problems,” *Appl. Math. Comput.*, vol. 147, no. 2, pp. 499–513, 2004.
- [37] A. Rehman, Z. Salleh, T. Gul, and Z. Zaheer, “The impact of viscous dissipation on the thin film unsteady flow of GO-EG/GO-W nanofluids,” *Mathematics*, vol. 7, no. 7, p. 653, 2019.
- [38] T. Gul, W. A. Khan, M. Tahir, R. Bilal, I. Khan, and K. S. Nisar, “Unsteady nano-liquid spray with thermal radiation comprising CNTs,” *Processes*, vol. 7, no. 4, p. 181, 2019.
- [39] N. S. Khan, T. Gul, S. Islam, I. Khan, A. M. Alqahtani, and A. S. Alshomrani, “Magnetohydrodynamic nanoliquid thin film sprayed on a stretching cylinder with heat transfer,” *Appl. Sci.*, vol. 7, no. 3, p. 271, 2017.
- [40] T. Gul, M. Z. Ullah, A. K. Alzahrani, and I. S. Amiri, “Thermal performance of the graphene oxide nanofluids flow in an upright channel through a permeable medium,” *IEEE Access*, vol. 7, pp. 102345–102355, 2019.